Orbital
The electronic journal of chemistry

the electronic journal of chemistry

Full Paper | http://dx.doi.org/10.17807/orbital.v16i4.21185

Synthesis and Characterization of Iron Oxide Nanoparticles by Using *Callistemon viminalis* Flowers Extract: An Eco-Friendly Approach with Promising Antioxidant Activities

Shweta Bansal, Ruchi Bharti*, Ajay Thakur, Monika Verma, and Renu Sharma

The present research article introduces a novel, environmentally friendly method for synthesizing ironoxide nanoparticles (IONPs) utilizing *Callistemon viminalis* flowers extract as both a reducing and capping agent. This approach not only offers a sustainable and cost-effective alternative to conventional synthesis methods but also harnesses the inherent phytochemical potential of the plant extract. The synthesized IONPs underwent comprehensive characterization using various analytical techniques including X-ray diffraction (XRD), scanning electron microscopy (SEM), Fourier-transform infrared spectroscopy (FTIR), and dynamic light scattering (DLS) to elucidate their structural, morphological, and chemical properties. Subsequently, the synthesized IONPs were evaluated for their potential antioxidant properties. The research findings contribute valuable insights into the synthesis process, structural characteristics, and antioxidant efficacy of the synthesized nanoparticles, offering promising avenues for addressing both health and environmental challenges with innovative solutions.

Graphical abstract

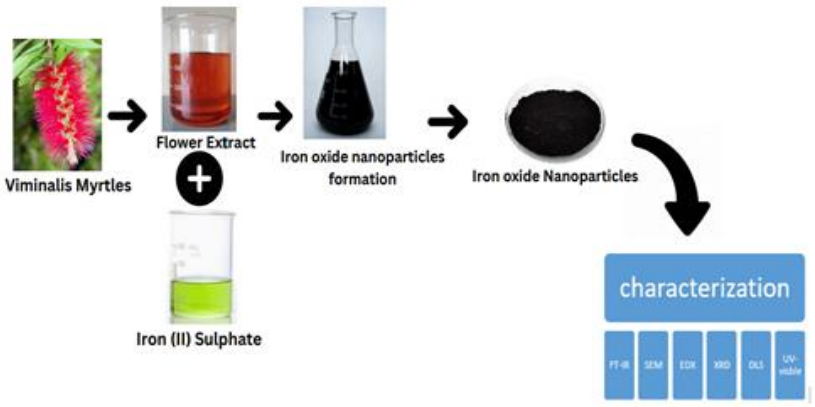

Keywords

Antioxidant activity
Environmentally friendly
Iron oxide nanoparticles (IONPs)
Callistemon viminalis

Article history

Received 20 May 2024
Revised 06 Jul 2024
Accepted 29 Jul 2024
Available online 03 Jan 2025

Handling Editor: Adilson Beatriz

1. Introduction

At its core, nanotechnology revolves around the creation and utilization of physical, chemical, and biological systems that operate on a minute scale, spanning from individual atoms or molecules to larger mesoscopic dimensions. This interdisciplinary field also involves integrating these nanomaterials into larger systems for various applications [1].

*Department of Chemistry, UIS, Chandigarh University, Gharuan, Mohali, Punjab-140413, India. *Corresponding author. E-mail: ruchi.uis@cumail.in

A pivotal challenge in nanotechnology lies in refining techniques for the precise synthesis of metal nanoparticles, ensuring meticulous controlover their size, shape, and composition [2]. Unlike their bulk counterparts, metal nanoparticles boast unique optical , magnetic [3], electronic, and catalytic properties [4], rendering them invaluable in a plethora of domains including biomedicine [5], optics, and electronics [3]. The exploration of these innovative applications underscores the transformative potential of metal nanoparticles in propelling scientific and technological progress [6-7]. Nanoparticles can be synthesized through various techniques, including chemical, electrochemical, photochemical, γ-radiation, laser ablation, and others [8-9]. However, these conventional methods often come with drawbacks, such as high costs and the generation of hazardous byproducts that can harm the environment. Moreover, the use of expensive chemicals and materials can result in uncertain shapes, sizes, and dispersions, further contributing to environmental pollution. In response to these challenges, biological methods are gaining traction as they offer a viable alternative. These methods are relatively simple to implement, involve less harmful chemical inputs during the synthesis process, and are ultimately cost-effective, leading to reduced pollution [10]. For the synthesis of (IONPs), *Callistemon viminalis*, commonly known as bottlebrush, is being utilized. This fragrant woody shrub is renowned for its aromatic qualities and boasts a wide range of biological and medicinal applications [11]. *Callistemon viminalis* extract exhibits antibacterial, antifungal, anticancer, anti-inflammatory, and anthelmintic properties, making it a valuable resource [12]. When it comes to synthesizing nanoparticles, *Callistemon viminalis* extract offers several advantages over other biological processes [11]. It is rich in polyphenols such as Tannins [13], flavonoids [14], which play a crucial role in the reduction and stabilization of nanoparticles [15]. Moreover, the use of *Callistemon viminalis* extract is environmentally friendly, as it produces no harmful byproducts during the synthesis process. Additionally, it can be easily scaled up for large-scale synthesis, making it a promising candidate for nanoparticle production [16]. Iron oxides represent a significant category of nanoparticles, comprising hematite (α-Fe_2O_3), maghemite (γ-Fe_2O_3), and magnetite (Fe_3O_4) [17]. These nanoparticles possess exceptional magnetic and electrical properties, including superparamagnetism, stability in liquid solutions, resistance to oxidation, and prolonged blood half-lives, rendering them valuable in various technological applications [18,19]. This study introduces a novel, environmentally friendly approach for the biosynthesis of IONPs using aqueous extracts obtained from the vibrant crimson flowers of *Callistemon viminalis*. Notably, this synthesis method eliminates the need for additional acids or bases, exemplifying a holistic and eco-conscious approach to IONP production [20]. To comprehensively characterize the synthesized iron nanoparticles, a range of analytical techniques will be employed, including UV-Visible spectroscopy, Fourier Transform Infrared (FTIR) spectroscopy, Scanning Electron Microscopy (SEM), Dynamic light scattering (DLS) and X-ray Diffraction (XRD). IONPs, have demonstrated versatility in various fields such as drug delivery systems, biomedicine, cosmetics, diagnostics, materials engineering, and adsorption of dyes, highlighting their multifunctional nature and potential for diverse applications [21, 22]. So this methodology is further contributing to the green synthesis of IONPs.

2. Material and Methods

Chemicals

The chemical reagents utilized in the study include Iron (II) Sulphate heptahydrate, 1,1-diphenyl-2-picrylhydrazyl (DPPH) , Dimethyl Sulfoxide and 2,2-azino-bis-(3-ethylbenzthiazoline-6-sulfonic acid) (ABTS), Methanol , Potassium persulfate (PPS), Ascorbic acid , Gallic acid. These reagents were procured from reputable suppliers such as Merck and Sigma-Aldrich, India, ensuring their high quality and reliability. By sourcing these reagents from established suppliers, we aimed to maintain the consistency and accuracy of the experimental outcomes obtained in this research endeavour. The use of high-quality reagents is essential for obtaining reliable results and ensuring the reproducibility of the experimental procedures conducted in this study.

2.2 Collection of Plant Material

The botanical material utilized in this study comprised *Callistemon viminalis flowers*, carefully assembled from the Chandigarh University, Mohali. The intentional selection of botanical specimens from this reputable botanical source enhances the credibility and authenticity of the experimental protocol, ensuring the reliability of the obtained findings. *Callistemon* is a genus of evergreen shrubs and small trees within the Myrtaceae family, native to Australia. These plants are renowned for their distinctive cylindrical flower spikes, resembling bottle brushes, hence the common name "Bottle Brush" (shown in Fig.1) The genus comprises various species, prized for their attractive flowers, resilience, and adaptability in landscaping. The hallmark feature of *Callistemon* is its unique inflorescence, characterized by dense clusters of bristly flowers arranged in cylindrical spikes.

Fig.1. *Callistemon viminalis* Myrtales.

Apart from their ornamental value, *Callistemon* species possess diverse medicinal properties, including antibacterial, antifungal, and antioxidant activities, along with pharmaceutical and insecticidal potential [23].

2.3 Preparation of *Callistemon viminalis* Myrtales extract

For the preparation of flower extract (shown in Fig. 2), flowers of the *C. viminalis* Myrtales plant were meticulously cleaned through multiple washing cycles to remove any impurities or contaminants. Subsequently, the cleaned flowers underwent a desiccation period lasting 5–6 days under ambient conditions, shielded from direct sunlight. Once thoroughly dried, the flowers were processed into a fine powder using a blender. In a 500 ml flask, 20g of the powdered flower material was combined with 400 ml of distilled water and heated to a gentle boil for 2 hours at 80 °C. Following the thermal treatment, the solution was allowed to cool to room temperature, after which it underwent filtration using Whatman filter paper to remove any solid residues.

2.4 Synthesis of Iron oxide nanoparticles

In the synthesis of IONPs as (shown in Fig. 2), Ferrous sulphate heptahydrate played a crucial role. A solution of Ferrous sulphate heptahydrate, with a concentration of 0.1 mM and a volume of 50 ml, was prepared for the synthesis process. This solution was adding dropwise into aqueous Callistemon viminalis extract at a volumetric ratio of 1.1 while maintaining temperature continuous stirring on a heating mantle at 100 °C.

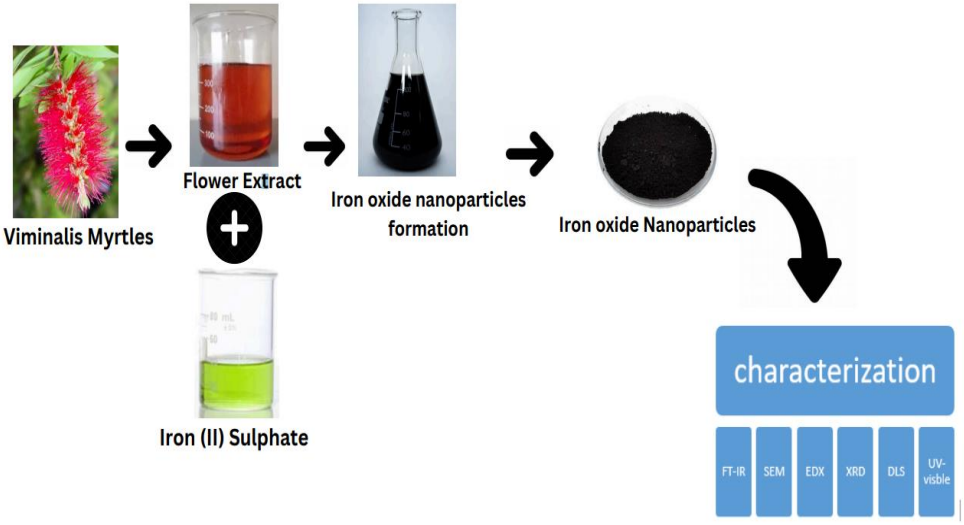

Fig. 2. Schematic representation of the IONPs biosynthesis mechanism.

The gradual addition of the plant extract facilitated the reduction of iron ions, resulting in the formation of a distinctive blue-colored solution. Following the reduction process, the solution underwent centrifugation at 1,000 rpm for 14 minutes to separate the upper liquid phase from the solid component. The solid residue, identified as IONPs, was then subjected to multiple washes using distilled water to remove any residual impurities. Finally, the washed IONPs were air-dried in an oven at 30°C for a period of 24 hours to obtain the final product.

2.5 Characterization

The characterization of the synthesized IONPs was conducted using a combination of analytical techniques, including Fourier-transform infrared spectroscopy (FTIR), scanning electron microscopy (SEM), dynamic light scattering (DLS), and X-ray diffraction (XRD) studies. FTIR analysis was employed to examine the chemical composition and functional groups present on the surface of the IONPs. This technique provides valuable insights into the bonding arrangements and molecular interactions within the nanoparticle structure. SEM imaging was utilized to investigate the morphology and surface topography of the IONPs. SEM allows for high-resolution imaging, enabling the visualization of the particle size, shape, and distribution. DLS analysis was employed to determine the size distribution and colloidal stability of the synthesized nanoparticles. By measuring the fluctuations in the intensity of scattered light, DLS provides information about the hydrodynamic diameter of the nanoparticles in solution. XRD studies were conducted to investigate the crystalline structure and phase composition of the IONPs. This technique enables the identification of crystallographic planes and lattice parameters, offering insights into the overall crystallinity and purity of the synthesized nanoparticles. Together, these characterization techniques offer a comprehensive understanding of the structural, morphological, and chemical properties of the synthesized IONPs.

3. Results and Discussion

Utilizing *Callistemon viminalis* flower extract, the synthesis of IONPs was precisely carried out through a carefully controlled procedure. Over the course of a carefully monitored three-hour reaction period, a visible transformation in color, shifting from a delicate red (shown in Fig.3a) to a profound shade of deep blue (shown in Fig.3b), clearly indicated the reduction of iron ions and the subsequent generation of IONPs (shown in Fig.3). This observable alteration in color not only served as a clear demonstration of the synthesis process but also validated findings documented in existing research concerning the formation of IONPs. Such alignment between the visual evidence and established scientific knowledge provided strong validation for the successful execution of the synthesis protocol.

3.1 FT-IR

The infrared (IR) spectra obtained from both the *Callistemon viminalis* flower extract and the synthesized IONPs offer valuable insights into their chemical compositions and structural characteristics. In the IR spectrum of the *Callistemon viminalis* flower extract (shown in Fig. 4), prominent peaks are observed at 3303 cm^{-1} and 1636 cm^{-1}, indicating the presence of O-H stretching vibrations associated with hydroxyl groups and C=C stretching vibrations characteristic of aromatic compounds, respectively. Conversely, the synthesized IONPs exhibit distinct peaks at various wavenumbers (Fig. 5). The peak at 3210 cm^{-1} suggests the presence of O-H stretching vibrations, possibly from residual water molecules or hydroxyl groups on the nanoparticle surface. Peaks at 1577 cm^{-1} and 1366 cm^{-1} indicate C=C stretching vibrations and C-N stretching

vibrations, respectively, implying the presence of organic compounds adsorbed on the nanoparticle surface. Additionally, peaks at 1068 cm^{-1}, 753 cm^{-1}, and 415 cm^{-1} correspond to Fe-O stretching and bending vibrations, confirming the presence of iron oxide bonds in the synthesized nanoparticles. Overall, the IR spectra provide comprehensive information about the chemical functionalities and structural properties of both the flower extract and the synthesized IONPs, facilitating a deeper understanding of their composition.

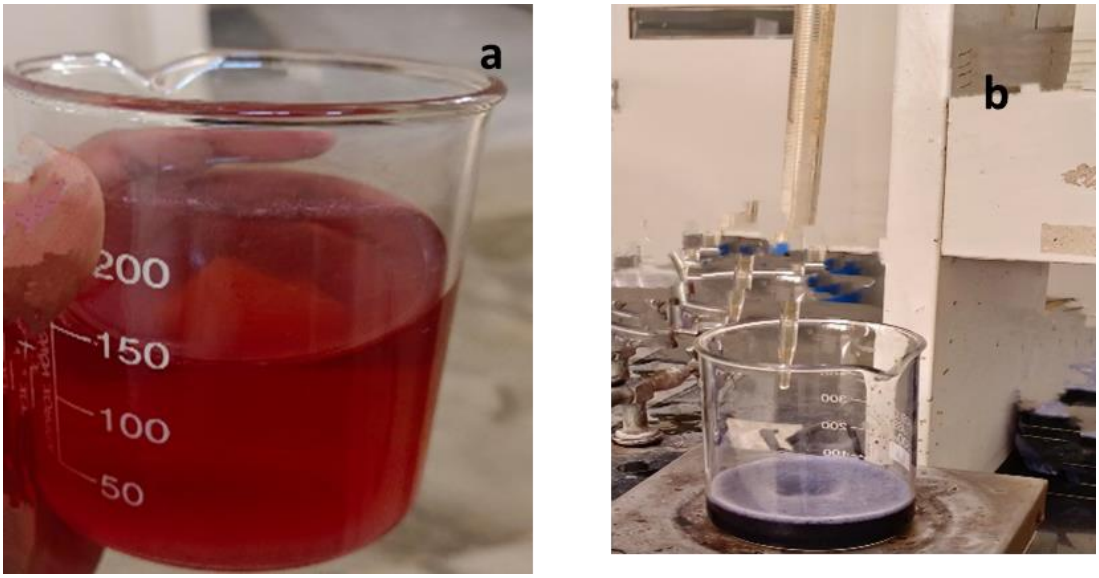

Fig. 3. (a) Flower extract of *Callistemon viminalis* and (b) reaction mixture containing $FeSO_4$ solution 0.1M and *Callistemon viminalis* flower extract.

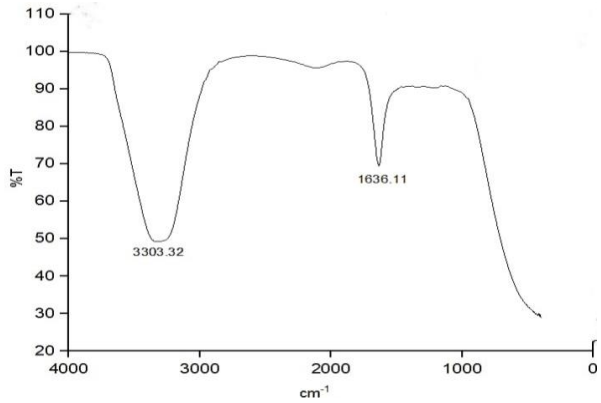

Fig. 4. FTIR spectrum of flower extract.

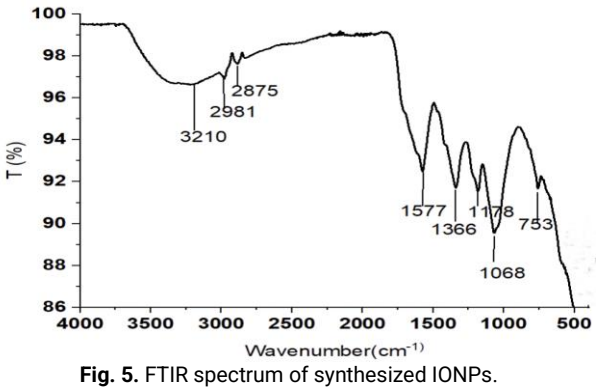

Fig. 5. FTIR spectrum of synthesized IONPs.

3.2 SED-EDX spectroscopy

Scanning Electron Microscopy with Energy Dispersive X-ray Spectroscopy is referred to as SEM-EDX. SEM provides detailed photographs of the topography of samples by enabling the visualization of their surfaces at high magnifications. However, by identifying the distinctive X-rays released when the sample is exposed to an electron bombardment in the SEM, EDX is utilized to determine the elemental composition of the sample. By combining SEM with EDX, materials' microstructures may be seen, and their constituent elements can be determined. The morphology analysis of the IONPs, as illustrated in (Fig. 6) depicts surface-uneven spherical particles, suggesting a heterogeneous size distribution rather than uniformity in size. While the spherical shape indicates a tendency towards symmetry, the uneven surface implies variations in particle size and surface roughness within the nanoparticle ensemble. Further elemental composition analysis of the IONPs reveals the presence of sulfur (S), oxygen (O), and iron (Fe) as primary constituents (Fig. 7). The sulfur content, constituting 5.50% of the composition, potentially indicates the presence of sulfur-based impurities. Oxygen, comprising 45.80% of the composition, is expected due to the formation of iron oxide bonds, reinforcing the synthesis of iron oxide nanoparticles. The predominance of iron, accounting for 48.70% of the composition, aligns with the intended synthesis and confirms the nanoparticle composition (Shown in Fig. 7). These findings collectively substantiate the successful synthesis of IONPs, validating the synthesis process and composition analysis.

3.3 Dynamic Light Scattering (DLS)

The obtained results (shown in Fig. 8) provide valuable insights into the size distribution and characteristics of the nanoparticles under investigation. The Z-average size of 280.1 nm suggests that the majority of particles in the sample have a mean hydrodynamic diameter around this value. The Polydispersity Index (PI) of 0.3283 indicates a moderate level of heterogeneity in particle size distribution, with some

variation observed among the particles. The intercept value of 0.9837 and a fit error of 0.0009533 demonstrate the reliability of the data obtained from the analysis, indicating a high degree of accuracy in the measurements. This ensures confidence in the reported particle sizes and distribution metrics. Furthermore, the analysis reveals that 91.17% of particles fall within the specified size range, indicating a relatively uniform distribution with the majority of particles exhibiting sizes within the expected range. The presence of two distinct peaks in the intensity-ordered mean peak sizes further highlights the complexity of the nanoparticle sample. Peak 1, with a mean size of 302.6 nm, likely represents one population of particles, while Peak 2, with a mean size of 521.8 nm, may correspond to another population or the presence of aggregates within the sample. This observation suggests the existence of multiple particle populations or varying sizes of aggregates, which could influence the sample's properties and behavior.

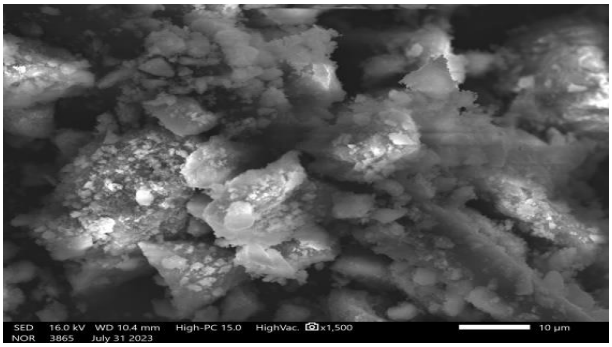

Fig. 6. SEM image of IONPs.

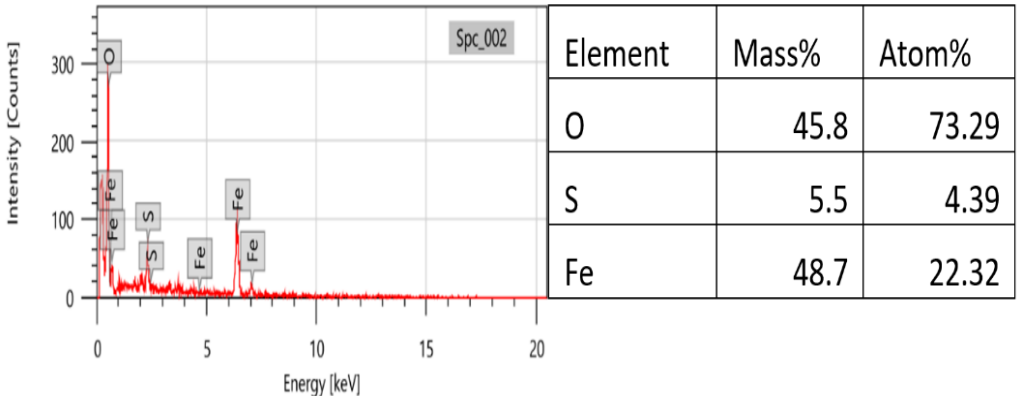

Element	Mass%	Atom%
O	45.8	73.29
S	5.5	4.39
Fe	48.7	22.32

Fig. 7. EDX spectrum of IONPs.

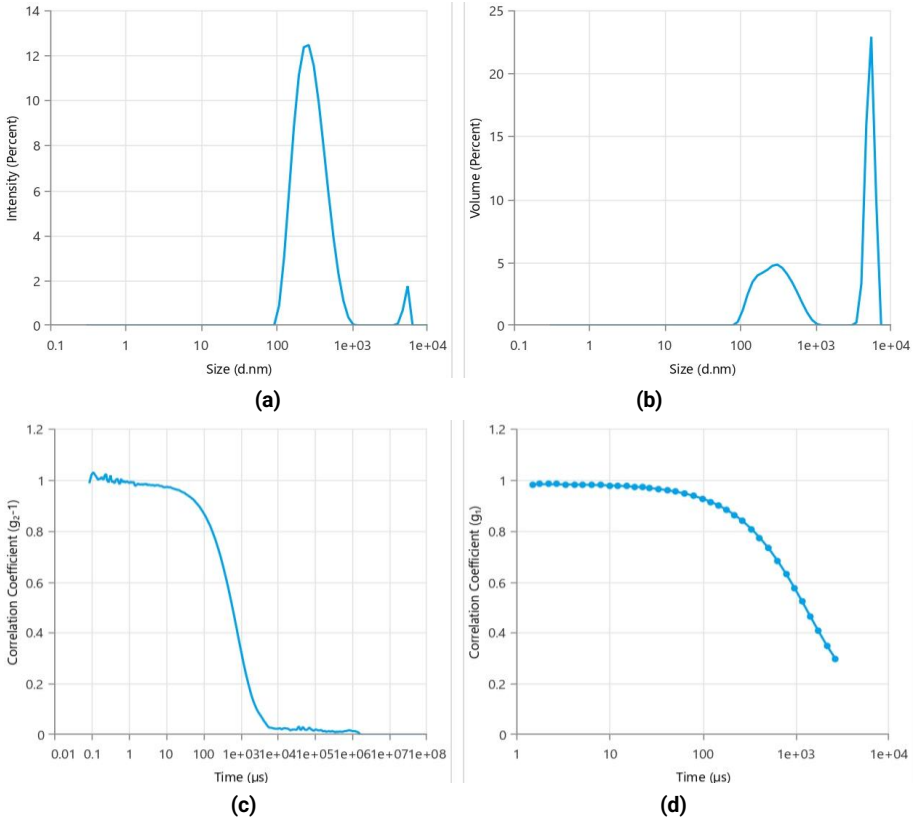

Fig. 8. (a, b) Size distribution and (c, d) Correlogram and Comulants fit diagram.

3.4 XRD

The X-ray diffraction (XRD) analysis of the synthesized IONPs revealed an amorphous nature, characterized by the absence of distinct peaks in the XRD pattern except for a single peak observed at 41.425° theta value. This absence of distinct peaks suggests that the nanoparticles lack a well-

defined crystalline structure, indicating an amorphous or disordered arrangement of atoms within the material. The presence of a solitary peak at 41.425° theta value could be attributed to a specific crystallographic plane or structural arrangement within the amorphous nanoparticles. However, the absence of additional peaks typically associated with crystalline materials implies a lack of long-range order or periodicity in the nanoparticle structure. This XRD analysis highlights the amorphous nature of the synthesized IONPs, highlighting their unique structural characteristics and distinguishing them from crystalline counterparts.

3.5 Anti-oxidant Activities

The antioxidant activity of IONPs was evaluated using the DPPH and ABTS assays, measuring the absorbance at 517 nm and 734 nm, respectively [24-26]. The experiments were conducted in triplicate, and the concentration of IONPs in the sample suspension was maintained at 1 mg/mL, prepared in dimethyl sulfoxide (DMSO). In the DPPH assay, IONPs exhibited a radical scavenging activity of 93.31% at an absorbance of 517 nm (shown in Table 1 and Fig. 9). This value indicates the percentage of DPPH radicals neutralized by the IONPs, demonstrating their potent antioxidant properties. Gallic acid, used as a standard reference, displayed a slightly higher radical scavenging activity of 91.76% ± 0.62%, while ascorbic acid exhibited an activity of 89.52% ± 0.89%. These results highlight the comparable antioxidant efficacy of IONPs to established antioxidant compounds. Similarly, in the ABTS assay conducted at 734 nm, IONPs demonstrated an impressive radical scavenging activity of 89.91% (shown in Table 1 and Fig. 9). This value reflects the percentage of ABTS radicals scavenged by the IONPs, further confirming their robust antioxidant activity. Gallic acid exhibited a higher radical scavenging activity of 96.53% ± 0.15%, while ascorbic acid showed an activity of 97.65% ± 0.15%. The high antioxidant activity of IONPs in both assays underscores their potential utility as effective antioxidants, with performance comparable to standard antioxidant compounds.

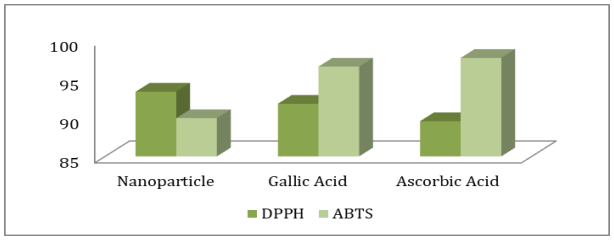

Fig. 9. Comparison of Antioxidant properties of synthesized IONPs.

The percentage (%) inhibition was calculated using relation given below:

$$\% [I] = [(A_{Control} - A_{Sample})/A_{Control}] \times 100$$

where $A_{Control}$ is the absorption of control and $A_{Control}$ is absorption of sample solution.

For ABTS:

$$\% [I] = [(0.748 - 0.050)/0.748] \times 100 = 93.31\%$$

For DPPH:

$$\% [I] = [0.585 - 0.059)/0.585] \times 100 = 89.91$$

Table 1. Antioxidant properties of IONPs.

	DPPH	ABTS
% (I) of IONPS	93.31	89.91
% (I) of Gallic Acid	91.76±0.62	96.53± 0.15
% (I) of Ascorbic Acid	89.52±0.89	97.65± 0.15
Control ($A_{control}$)	0.748	0.585
S1	0.052	0.058
S2	0.050	0.061
S3	0.049	0.059
Sample (A_{sample})	0.050	0.059

DPPH: 1, 1- diphenyl-2-picrylhydrazyl andABTS: 2 and 2-azino-bis- (3- ethylbenzthiazoline-6-sulfonic acid) . Values are means of three replicates ± standard deviation of the mean.

4. Conclusions

In conclusion, the synthesis of IONPs using *Callistemon viminalis* flower extract yielded promising results, demonstrating effective nanoparticle generation without the need for hazardous chemicals. Characterization techniques confirmed the successful synthesis, revealing the amorphous nature of the nanoparticles. Furthermore, the IONPs exhibited potent antioxidant activity, comparable to standard antioxidants. Importantly, this eco-friendly synthesis approach utilizing plant extract highlights the sustainable and cost-effective nature of the methodology, underscoring its advantages in nanomaterial synthesis. This study contributes to advancing nanotechnology with a bioinspired, environmentally friendly approach, offering potential applications across various fields.

Acknowledgments

We are thankful to Chandigarh University because this research was supported by the Department of Chemistry, Chandigarh University.

Author Contributions

Shweta Bansal: Methodology, Writing - Original Draft; Ruchi Bharti: Conceptualization, Supervision, Project Administration; Ajay Thakur: Data Curation; Monika Verma: Investigation, Formal Analysis; Renu Sharma: Resources, Visualization.

References and Notes

[1] Nasrollahzadeh, M.; Sajadi, S. M.; Sajjadi, M.; & Issaabadi, Z. An introduction to nanotechnology. In Interface science and technology. Elsevier, 2019. Vol. 28, pp. 1-27.

[2] Szczyglewska, P.; Feliczak-Guzik, A.; & Nowak, I. *Molecules* **2023**, *28*, 4932. [Crossref]

[3] Trügler, A. Optical properties of metallic nanoparticles: basic principles and simulation. Springer, 2016. Vol. 232.

[4] Ahmadi, M.; Mistry, H.; & Roldan Cuenya, B. *J. Phys. Chem. Lett.* **2016**, *7*, 3519. [Crossref]

[5] Bhattacharya, R.; & Mukherjee, P. *Adv. Drug Deliv. Rev.* **2008**, *60*, 1289. [Crossref]

[6] Thakur, A.; Verma, M.; Bharti, R.; Sharma, R. *Curr. Chin.*

Sci. **2023**, *3*, 322. [Crossref]

[7] Jamkhande, P. G.; Ghule, N. W.; Bamer, A. H.; & Kalaskar, M. G. *J. Drug Deliv. Sci. Technol.* **2019** , *53*, 101174. [Crossref]

[8] Mazumdar, H.; & Haloi, N. *J. Microbiol. Biotechnol. Res.* **2011**, *1*, 39.

[9] Dhand, C.; Dwivedi, N.; Loh, X. J.; Ying, A. N. J.; Verma, N. K.; Beuerman, R. W.; Rajamani L.; Ramakrishna, S. *RSC Adv.* **2015**, *5*, 105003. [Crossref]

[10] Pattanayak, D. S.; Pal, D.; Thakur, C.; Kumar, S.; & Devnani, G. L. *Mater. Today Proc.* **2021**, *44*, 3150. [Crossref]

[11] Abdelhady, M. I.; Abdou, R.; Bamagous, G. A.; Elshahat, M.; & Barghash, M. F. *Appl. Sci. Rep.* **2015**, *11*, 22. [Crossref]

[12] Uwaya, G. E.; Fayemi, O. E.; Sherif, E. S. M.; Junaedi, H.; Ebenso, E. E. *Materials* **2020**, *13*, 4894. [Crossref]

[13] Marzouk, M. S. *Phytochem. Anal.* **2008**, *19*, 541. [Crossref]

[14] Ahmed, K. Z.; Naeem, S.; Noo, A. *Ann Jinnah Sindh Med. Uni.* **2018**, *4*, 4.

[15] Mahgoub, S.; Hashad, N.; Ali, S.; Ibrahim, R.; Said, A. M.; Moharram, F. A.; Mady, M. *Molecules* **2021**, *26*, 2481. [Crossref]

[16] Rahisuddin, Akrema. *Spectrosc. Lett.* **2016**, *49*, 268. [Crossref]

[17] Kanagesan, S.; Hashim, M.; Tamilselvan, S.; Alitheen, N. B.; Ismail, I.; Hajalilou, A.; & Ahsanul, K. *Adv. Mater. Sci. Eng.* **2013**, *21*, 312. [Crossref]

[18] Sundaram, P. A.; Augustine, R.; Kannan, M. *Biotechnol. Bioprocess Eng.* **2012**, *17*, 835. [Crossref]

[19] Priya, Naveen, Kaur, K.; & Sidhu, A. K. *Front. Nanotechnol***. 2021**, *3*, 655062. [Crossref]

[20] Hassan, D., Khalil, A. T.; Saleem, J.; Diallo, A.; Khamlich, S.; Shinwari, Z. K.; Maaza, M. *Artif. cells Nanomed. Biotechnol.* **2018,** *46*, 693. [Crossref]

[21] De França Bettencourt, G. M.; Degenhardt, J.; Torres, L. A. Z.; de Andrade Tanobe, V. O.; Soccol, C. R. *Biocatal. Agric. Biotechnol.* **2020**, *30*, 101822. [Crossref]

[22] Khalil, A. T.; Ovais, M., Ullah, I.; Ali, M., Shinwari, Z. K.; Maaza, M. *Green Chem. Lett. Rev.* **2017**, *10*, 186. [Crossref]

[23] Oyedeji, O. O.; Lawal, O. A.; Shode, F. O.; Oyedeji, A. O. *Molecules* **2009**, *14,* 1990. [Crossref]

[24] Thakur, A.; Bharti, R.; Verma, M.; Sharma, R.; Sharma, A.; Gupta, A.; Sharma, V. *Synthesis* **2023**, *55*, 3129. [Crossref]

[25] Verma, M.; Thakur, A.; Kapil, S.; Sharma, R.; Sharma, A.; Bharti, R. *Mol. Divers.* **2023**, *27*, 889. [Crossref]

[26] Thakur, A.; Verma, M.; Setia, P.; Bharti, R.; Sharma, R.; Sharma, A.; Bansal, R. *Res. Chem. Intem.* **2023**, *49*, 859. [Crossref]

How to cite this article

Bansal, S.; Bharti, R.; Thakur, A.; Verma, M.; Sharma, R. *Orbital: Electron. J. Chem.* **2024**, *16*, 240. DOI: **http://dx.doi.org/10.17807/orbital.v16i4.21185**